*International Journal of Marine Engineering Innovation and Research, Vol. 11(2), Jun. 2026. 517-525*
*(pISSN: 2541-5972, eISSN: 2548-1479)*



# Study on Kalina Cycle Performance Under Operating Temperature Variations for Ship Waste Heat Recovery

Thashya Nabila Aqeela[1], Fajri Ashfi Rayhan [2*]

(Received: 30 April 2026 / Revised: 2 May 2026 / Accepted: 11 May 2026 / Available Online: 8 June 2026)

***Abstract*—** Energy inefficiency in marine diesel engines remains a significant challenge due to substantial waste heat losses. This study aims to evaluate the thermodynamic performance of a Kalina cycle for waste heat recovery from a low-speed marine diesel engine under varying operating temperature and ammonia-$H_2O$ compositions. A thermodynamic model is developed based on mass and energy balance principles to analyze system behavior under different conditions. The analysis focuses on key performance parameters, including evaporator heat input ($Q_{in}$), pump work, expander work, thermal efficiency, and energy losses for ammonia concentrations of 30%, 45%, and 60%. The results show that increasing ammonia concentration significantly reduces the required heat input, while expander work decreases with rising condenser temperature due to a reduced enthalpy drop. Thermal efficiency decreases with increasing evaporator temperature, as additional heat input is not effectively converted into useful work, resulting in greater irreversibility. The highest efficiency of 11.9% is achieved at 60% ammonia concentration under lower temperature conditions. In contrast, energy losses increase consistently with higher heat input, particularly at elevated temperatures. The performance of the Kalina cycle is strongly influenced by operating temperatures and working fluid composition, providing insight for optimizing the marine waste heat recovery system.

*Keywords*—*Kalina cycle;* Ammonia-$H_2O$ mixture; thermal efficiency; waste heat recovery

[*]*Correspodning Author: fajri.ar@upnvj.ac.id*

## I. INTRODUCTION[1]

Energy efficiency has become a critical concern in the maritime sector, where low-speed marine diesel engines remain the dominant propulsion technology. Despite their high reliability and operational robustness, a substantial portion of the fuel energy cannot be effectively converted into useful mechanical work. It is estimated that approximately 50% of the total energy released during the combustion process is dissipated as waste heat through exhaust gases and the cooling system [1]. In addition, transportation accounted for approximately 2.89% of global $CO_2$ emissions in 2018 [2]. These challenges necessitate the development of advanced energy recovery technologies to enhance overall system efficiency while mitigating environmental impact.

The Kalina cycle is considered a promising technology for recovering waste heat and converting it into additional power output, especially for low- to medium-temperature heat sources. The cycle comprises several key components: an evaporator as the primary heat exchanger, a separator for phase separation of the working fluid, an expander for converting thermal energy into mechanical work, a condenser for heat rejection, and a pump to ensure continuous fluid circulation within the system. One of the major advantages of the Kalina cycle is its capability to maintain better temperature compatibility between the heat source and the working fluid during the evaporation process. This characteristic enables improved utilization of low- and medium-temperature waste heat, which is generally difficult to recover using a Rankine cycle. This capability allows for enhanced thermal efficiency under conditions where other cycles exhibit limited performance [3]. Moreover, the implementation of the Kalina cycle contributes to fuel savings while simultaneously reducing emissions, highlighting its potential as an environmentally sustainable solution, particularly in maritime applications [4].

Previous studies have examined the thermodynamic behavior of the Kalina cycle under various operating conditions for waste-heat recovery applications. Larsen et al. [5] reported that the Kalina cycle has strong potential for marine waste heat recovery due to its superior thermal matching between the heat source and the working fluid. Ngunyen et al. [6] further demonstrated that variations in ammonia-$H_2O$ concentration significantly influence heat transfer characteristics and cycle efficiency. In addition, Hossain et al. [7] showed that operating temperature and pressure strongly affect exergy destruction and overall thermodynamic performance, particularly within the evaporator and expander components. Comparative studies by Bombarda et al. [8] also indicated that the Kalina cycle can achieve better performance than conventional Organic Rankine Cycles (ORC) under low- and medium-temperature waste heat conditions due to its non-isothermal phase change and optimization strategies. Detailed investigations regarding component-level energy distribution and thermodynamic losses under varying operating temperatures and ammonia-$H_2O$

Thashya Nabila Aqeela, Naval Architecture, Faculty of Engineering, Universitas Pembangunan Nasional Veteran Jakarta, Indonesia. E-mail: 2210313063@mahasiswa.upnvj.ac.id
Fajri Ashfi Rayhan, Naval Architecture, Faculty of Engineering, Universitas Pembangunan Nasional Veteran Jakarta, Indonesia. E-mail: fajri.ar@upnvj.ac.id

compositions remain limited, especially for marine low-speed diesel engine applications.

Feng et al [1] demonstrated that the Kalina cycle has significant potential for optimizing low- to medium-temperature waste heat recovery. Their thermodynamic simulation on a MAN 8S90ME-C10.2 marine diesel engine showed that integrating the Kalina cycle with a supercritical $CO_2$ Brayton cycle can increase energy efficiency by up to 16.62% and reduce $CO_2$ emissions by 15.01%. In addition, the superior performance of the Kalina cycle is strongly attributed to the thermophysical properties of the ammonia-$H_2O$ mixture, which enables non-isothermal phase change over a temperature range. This characteristic enhances heat transfer effectiveness and improves temperature matching between the heat source and working fluid, resulting in more efficient energy utilization compared to systems employing pure fluids [9][10].

However, Feng et al [1] primarily focused on overall system performance and did not provide a detailed assessment of energy distribution across individual components of the Kalina cycle. Critical parameters, including evaporator heat input ($Q_{in}$), pump work consumption, and internal energy losses, were not explicitly quantified. These parameters are essential for accurately characterizing system performance, as they directly govern energy efficiency and reflect the magnitude of thermodynamic losses occurring throughout the cycle.

Accordingly, the study aims to conduct a thermodynamic analysis of a Kalina cycle integrated with a low-speed diesel engine under varying operating temperatures and ammonia-$H_2O$ compositions. The analysis focuses on evaluating energy distribution across major system components, including heat transfer characteristics, work interactions, and associated losses. The findings are expected to provide deeper insight into system behavior and support optimization of waste heat recovery performance in marine energy systems.

## II. METHOD

### *A. Initial and Boundary Conditions*

In this study, a Kalina cycle is integrated with a marine low-speed diesel engine (MAN B&W 8S90ME-C10.2) as the primary heat source. The waste heat recovered from the exhaust gas is utilized to drive the thermodynamic cycle for additional power generation. The thermodynamic properties of the ammonia-$H_2O$ working fluid are evaluated using REFPROP, ensuring accurate evaluation across varying operating conditions.

### *B. Kalina Cycle System Schematic*

The schematic configuration of the Kalina cycle employed in this study is presented in Figure 1. The system consists of key components, including an evaporator, separator, expander, mixer, condenser, pump, regenerator, and throttle valve, which operate in an integrated manner to maintain continuous thermodynamic performance.

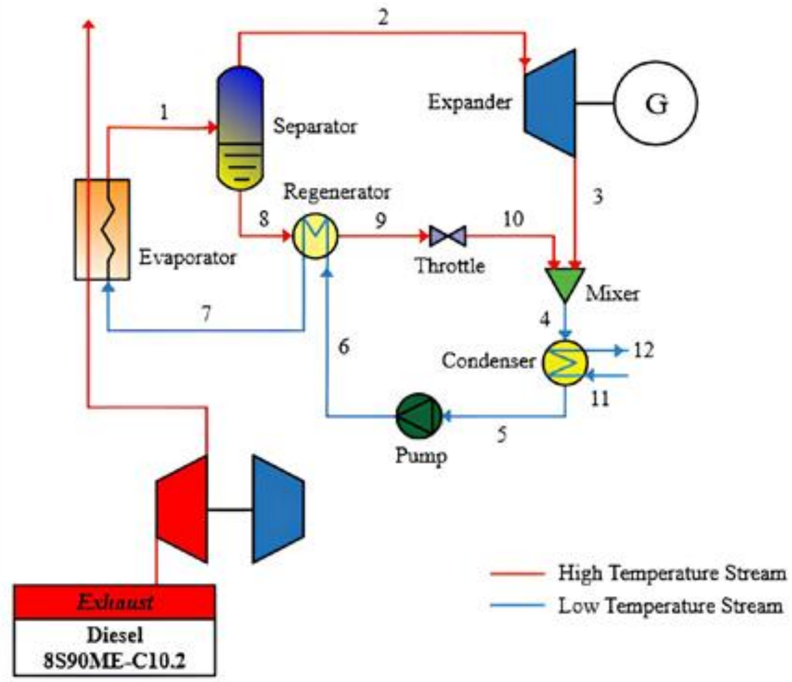


**Figure 1.** Kalina Cycle System Schematic

The Kalina cycle operating begins in the evaporator, where the working fluid absorbs heat from the exhaust gas and is converted into a vapor-liquid mixture. The mixture then enters the separator (1), where it is separated into vapor and liquid phases. The vapor stream is directed to the expander (2), where it expands to generate mechanical power.

The low-pressure vapor exiting the expander subsequently flows into the mixer (3). In parallel, the liquid stream from the separator is routed through the regenerator (8) after passing a throttle valve (9), where the pressure is reduced under isenthalpic conditions. The preheated liquid stream is then directed to the mixer (10).

In the mixer, the vapor and liquid streams are combined to achieve thermal and pressure equilibrium before entering the condenser (4). Within the condenser, the mixture of low-pressure vapor and liquid is cooled by the cooling water streams (11 and 12), resulting in complete condensation of the working fluid into liquid form. The condensed fluid is then pressurized by the pump (5) and directed to the regenerator (6), where it absorbs residual heat from the cycle. Finally, working fluid flows back to the evaporator (7) to absorb heat from the exhaust gas, thereby completing a continuous closed-loop cycle.

### *C. Parameters Analysis*

A consistent set of boundary conditions and component-level performance parameters is defined to support the thermodynamic analysis, see Table 1.

TABLE 1.
SYSTEM OPERATING PARAMETERS

| Parameters | Value |
|---|---|
| Inlet mass flow (kg/s) | 90.49 |
| Inlet temperature (°C) | ~270 |
| Expander inlet pressure (MPa) | 2~4 |
| Condenser outlet temperature (°C) | 28~32 |
| Expander adiabatic efficiency (%) | 80~100 |
| Pump adiabatic efficiency (%) | 70~90 |
| Regenerator temperature difference (°C) | 7~9 |
| Evaporator outlet temperature (°C) | 179~184 |
| Cooling water inlet temperature (°C) | 20~30 |
| Cooling water outlet temperature (°C) | 20~30 |
| Working Fluid | Ammonia & $H_2O$ |
| Ammonia Percentage | 30%, 45%, and 60% |

### *D. Operating Parameters*

The thermodynamic model of the Kalina cycle is developed based on mass and energy balance principles applied to each component within the system, as described in the following equations.

$$\eta_{is,pump} = \frac{(h_{6s} - h_5)}{(h_6 - h_5)} \tag{1}$$

Equation (1) represents the isentropic efficiency of the pump. $h_5$ is the specific enthalpy at the pump inlet, $h_6$ is the actual enthalpy at the pump outlet, and $h_{6s}$ is the enthalpy at the pump outlet under isentropic conditions. This equation reflects the pump's performance and its deviation from ideal conditions.

$$Q_{evaporator} = m\,(h_1 - h_7) \tag{2}$$

Equation (2) defines the heat input in the evaporator, where $m$ is the mass flow rate, while $h_1$ and $h_7$ represent the outlet and inlet enthalpies of the evaporator. This relation quantifies the thermal energy absorbed from the exhaust gas and serves as the key parameter in assessing the effectiveness of waste heat utilization.

$$m_1 h_1 = m_2 h_2 + m_8 h_8 \tag{3}$$

Equation (3) represents the energy balance within the separator, where $m_1$, $m_2$, and $m_8$ denote the mass flow rates, while $h_1$, $h_2$, and $h_8$ are the corresponding enthalpies. This equation ensures energy conservation, ensures phase separation, and governs the distribution of vapor and liquid streams in the system.

$$W_{expander} = m_2(h_2 - h_3) \tag{4}$$

Equation (4) defines the mechanical power output generated by the expander, where $m_2$ is the vapor mass flow rate and $h_2$ and $h_3$ represent the inlet and outlet enthalpies. This equation captures the primary energy conversion process and directly determines the cycle's power generation capacity.

$$m_4 h_4 = m_3 h_3 + m_{10} h_{10} \tag{5}$$

Equation (5) describes the energy balance in the mixer, where $m_3$ and $m_{10}$ are the inlet mass flow rates and $m_4$ is the total mass flow rate, with corresponding enthalpies $h_3$, $h_{10}$, and $h_4$. This relation ensures thermodynamic consistency during the mixing process before condensation.

$$Q_{condenser} = m_4(h_4 - h_5) \tag{6}$$

Equation (6) quantifies the heat rejected in the condenser, where $m_4$ is the mass flow rate and $h_4$ and $h_5$ denote the inlet and outlet enthalpies. This equation is essential for evaluating heat dissipation to the cooling medium and its influence on system performance.

$$W_{pump} = m_5(h_6 - h_5) \tag{7}$$

Equation (7) represents the work required by the pump, where $m_5$ is the mass flow rate, $h_5$ and $h_6$ are the inlet and outlet enthalpies. This term accounts for the energy input necessary to maintain continuous circulation of the working fluid.

$$Q_{regenerator} = m_6(h_7 - h_6) = m_8(h_8 - h_9 \quad (8)$$

Equation (8) describes the heat exchange process within the regenerator, where $m_6$ and $m_8$ represent the mass flow rates of the cold and hot streams, and $h_6$, $h_7$, $h_8$, and $h_9$ denote their respective enthalpies. This formulation accounts for internal heat recovery, which enhances the cycle's overall thermodynamic efficiency.

$$h_9 = h_{10} \quad (9)$$

Equation (9) represents the throttling process, which is assumed to be isenthalpic. The equality of enthalpy indicates that no heat or work is transferred across the valve during pressure reduction.

$$W_{net,KC} = W_{expander} - W_{pump} \quad (10)$$

Equation (10) defines the net power output of the Kalina cycle as the difference between the expander work and pump work. This expression represents the actual useful power delivered by the system.

$$\eta_{n,KC} = \frac{W_{net,KC}}{Q_{evaporator}} \quad (11)$$

Equation (11) expresses the thermal efficiency of the cycle as the ratio of the net power output to heat input. This equation serves as a key indicator of the system's ability to convert thermal energy into useful work.

$$W_{Loss} = \left(1 - \eta_{n,KC}\right) Q_{evaporator} \quad (12)$$

Equation (12) represents the energy losses within the system, where $W_{Loss}$ corresponds to the portion of input heat that is not converted into useful work due to irreversibilities. This formulation is essential for identifying inefficiencies and guiding performance optimization.

## III. Results and Discussion

### A. Evaporator Heat Input

The evaporator heat input ($Q_{in}$) represents the thermal energy absorbed by the working fluid to facilitate phase transition from liquid to vapor. As shown in Figure 2, $Q_{in}$ increases with rising evaporator inlet temperature from 179°C to 184°C across all ammonia concentrations.

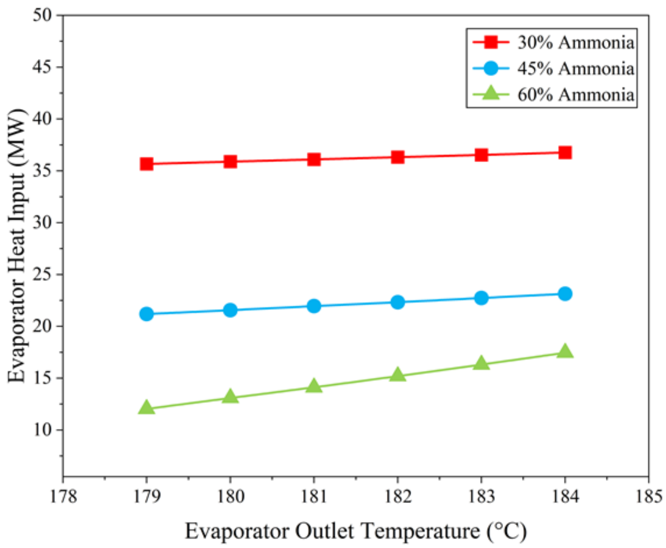


**Figure 2.** Heat input respons to evaporator outlet temperatures at different ammonia concentrations

At 30% ammonia concentration, $Q_{in}$ ranges from 35.67 MW to 36.77 MW, showing a relatively mild increase. This behavior is attributed to the higher water content, which possesses a large specific heat capacity, resulting in a greater portion of energy being utilized for sensible heating rather than phase change [9]. At 45% concentration, Qin ranges from 21.19 MW to 23.14 MW, with a more pronounced increase with temperature. This indicates a stronger thermodynamic response due to the higher ammonia fraction [11]. At 60% ammonia concentration, the lowest $Q_{in}$ values are observed, ranging from 12.03 MW to 17.46 MW, but with the steepest increase. This trend is associated with the higher volatility of ammonia, which accelerates phase transition and amplifies energy variation [12].

These results indicate that working fluid composition significantly affects heat absorption characteristics, which directly influence overall system energy requirements.

### B. Pump Work

The mechanical energy required to elevate the working fluid pressure from the condenser outlet to the evaporator inlet is represented by the pump work. As depicted in Figure 3, the required pump work decreases with increasing pump inlet temperature from 28°C to 32°C for all ammonia concentrations.

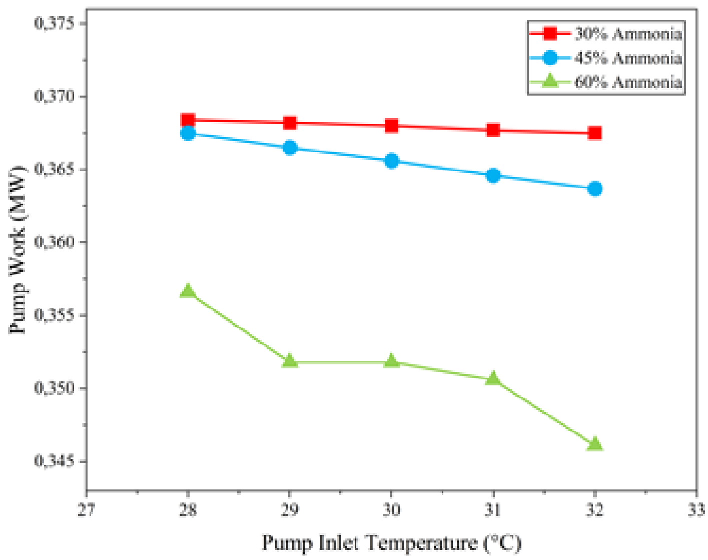


**Figure 3.** Effect of pump inlet temperature on pump work at different ammonia concentrations

At a 30% ammonia concentration, pump work decreases slightly from 0.3684 MW to 0.3675 MW, indicating low sensitivity to temperature variation. At 45% concentration, a more noticeable reduction is observed, with values decreasing from 0.3675 MW to 0.3637 MW. The most significant decrease occurs at 60% ammonia concentration, where pump work declines from 0.3566 MW to 0.3461 MW.

This phenomenon is primarily associated with variations in the thermodynamic properties of the ammonia-$H_2O$ mixture, particularly the enthalpy difference across the pump. Under certain operating conditions, nearly identical pump work values are obtained due to minimal differences between inlet and outlet enthalpy. These results suggest that pump performance is predominantly governed by pressure and enthalpy variations rather than temperature alone [13].

In addition to affecting pump behavior, ammonia concentration also significantly influences expander performance and overall cycle output. Increasing the ammonia fraction enhances vapor generation and increases the mass flow rate through the expander, which contributes to higher power output up to an optimal concentration. At higher concentrations, further increases tend to intensify thermodynamic irreversibilities, thereby reducing the effectiveness of energy conversion. This indicates the presence of a trade-off between maximizing power output and maintaining efficient heat utilization within the cycle [14][11].

Despite these variations, the overall contribution of pump work to the net cycle output remains relatively small compared to expander work. Therefore, although optimizing pump performance can improve system efficiency, its overall impact is generally less significant than that of high-energy components such as the expander. Consequently, greater attention is typically directed toward optimizing components with larger energy contributions, while still considering pump performance within the overall system design [15].

### C. *Expander Work*

Expander work constitutes the primary source of power generation in the Kalina cycle, where the thermal energy of the working fluid is converted into mechanical output through expansion. As presented in Figure 3, the expander output consistently decreases with increasing condenser temperature from 28°C to 32°C for each ammonia concentration.

At an ammonia concentration of 30%, the expander work decreases from 3.4 MW to 3.27 MW. A comparable trend is observed at 45% concentration, with values declining from 2.52 MW to 2.39 MW. At 60% ammonia concentration, the expander output further decreases from 1.84 MW to 1.72 MW, confirming a consistent reduction in power generation with rising condenser temperature.

The reduction in expander output can be explained by the smaller enthalpy difference between the inlet and outlet states as the condenser temperature increases. An increase in condenser temperature raises the outlet enthalpy of the working fluid, thereby reducing the available energy for expansion. As a result, the mechanical work produced by the expander decreases, which contributes to the overall decline in cycle performance, consistent with previous thermodynamic analyses under varying condenser conditions [16].

The influence of ammonia concentration is also evident in expander performance. Lower ammonia concentrations tend to produce higher expander work due to more favorable expansion characteristics, whereas higher concentrations, although beneficial for heat absorption, reduce the effective work output. This indicates a thermodynamic trade-off between heat recovery capability and power generation efficiency within the cycle.

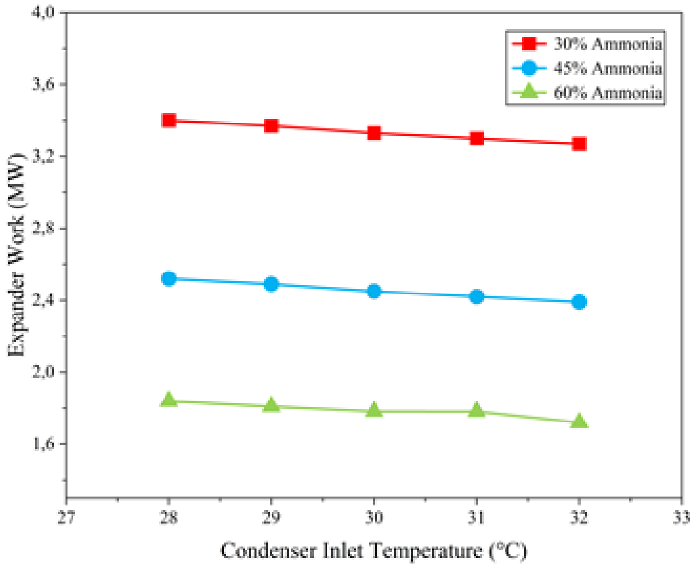


**Figure 4.** Expander work at different condenser inlet temperatures and ammonia concentrations

A relatively minor variation in expander work is observed at 60% ammonia concentration within the temperature range of 30°C to 31°C. This suggests that the enthalpy difference across the expander remains nearly constant under these conditions, leading to only slight changes in output. Such behavior reinforces the principle that expander performance is predominantly governed by enthalpy variation rather than temperature alone.

Given its dominant contribution to net cycle output, the expander plays a decisive role in determining overall system performance. Therefore, optimizing key operating parameters, particularly condenser temperature and working fluid composition, is essential to maximize power output and enhance the overall efficiency of the Kalina cycle [15].

*D. Thermal Efficiency*

The Kalina cycle's capacity to convert heat into useful mechanical work is quantified by its thermal efficiency. As illustrated in Figure 5, there is a discernible reduction in thermal efficiency as the evaporator inlet temperature is scaled from 179°C to 184°C for all ammonia concentrations. This behavior is not merely a consequence of higher heat input, but rather indicates a shift in the thermodynamic balance toward greater exergy destruction within the system, particularly in the evaporator [17].

At lower ammonia concentration (30%), the reduction in efficiency is relatively small, decreasing from 8.3% to 8.07%, suggesting that the system remains less sensitive to temperature-induced irreversibility under water-rich conditions. However, as the ammonia fraction increases, the decline becomes more pronounced. At 45%, efficiency drops from 9.8% to 9.1%, while at 60%, it decreases sharply from 11.9% to 8.2%. This indicates that although higher ammonia concentrations enhance efficiency at lower temperatures, they also amplify the system’s sensitivity to thermal conditions, particularly when operating beyond the optimal range [18].

This trend is fundamentally linked to the disparity between heat absorption and work production. Raising the evaporator temperature significantly increases the heat input, yet the expansion process cannot effectively capture this additional energy. Instead, a growing portion of this energy is degraded due to irreversibility, especially in the evaporation process, where temperature gradients and phase-change effects become more dominant [19]. Similar findings have been reported in advanced Kalina cycle configurations, where efficiency improves only up to an optimal combination of temperature and operating conditions, beyond which further increases primarily contribute to exergy destruction rather than useful work output [7].

The role of ammonia concentration further reinforces this interpretation. Ammonia-rich mixtures provide better thermal matching and heat absorption at moderate temperatures, leading to higher efficiency under optimal conditions. However, at elevated temperatures, these mixtures become more susceptible to thermal mismatches and complex phase behavior in the evaporator and separator, which intensifies irreversibility and reduces performance [20]. This explains why the highest efficiency is achieved at 60% ammonia concentration only at the lower evaporator temperature, rather than at higher thermal input levels.

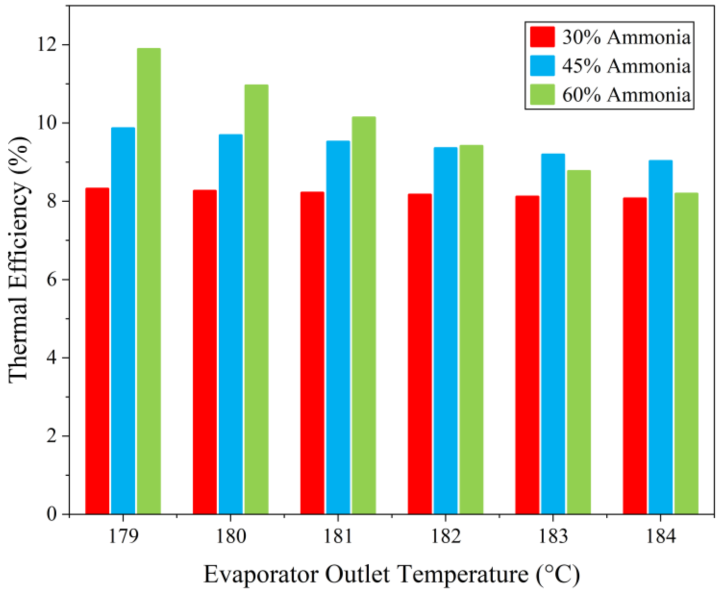


**Figure 5.** Thermal efficiency variation with evaporator outlet temperature at different ammonia concentrations

Compared to previous studies, an improvement of approximately 3.8% in thermal efficiency is achieved relative to Feng et al [1], under conditions of 179°C and 60% ammonia concentration. This improvement highlights that performance gains are primarily driven by better alignment between operating conditions and working-fluid properties, rather than by increasing the heat source temperature alone. Similar incremental improvements have been reported in optimized Kalina systems, where efficiency gains are obtained through coordinated adjustment of system parameters rather than increasing thermal input [21]. These findings indicate that proper selection of ammonia concentration and operating temperature is essential to achieve efficient energy conversion while minimizing thermodynamic losses.

*E. Energy Losses*

Energy losses in the Kalina cycle are the fraction of thermal energy that fails to be converted into work, largely due to inherent irreversibilities in expansion and heat transfer. As shown in Figure 6, increasing the evaporator inlet temperature from 179°C to 184°C results in a consistent increase in energy losses across all ammonia concentrations. This trend reflects a fundamental thermodynamic limitation, where additional heat input at higher temperatures results in disproportionately higher exergy destruction [17].

At 30% ammonia concentration, the heat input increases from 32.7 MW to 33.8 MW. A similar trend is observed at 45% concentration, where the heat input rises from 19.1 MW to 21.05 MW. The most pronounced increase occurs at 60% ammonia concentration, with values rising from 10.6 MW to 16.03 MW. The sharper increase at higher ammonia concentration suggests that ammonia-rich mixtures are more sensitive to temperature elevation, particularly in terms of irreversibility generation [18].

This behavior can be understood by examining the role of heat exchangers within the cycle. Previous studies consistently identify the evaporator and related heat exchange components as the primary sources of exergy destruction, due to finite temperature differences and non-ideal phase-change processes [7][21][22]. As the evaporator temperature increases, more energy is introduced into these components; however, the system's ability to utilize this energy does not increase proportionally. Instead, a larger fraction is dissipated before reaching the expander, resulting in higher overall energy losses [19].

The influence of ammonia concentration further intensifies this effect. Higher ammonia fractions enhance heat absorption and initially improve performance, but they also increase sensitivity to thermal mismatches and phase-equilibrium limitations at elevated temperatures. This leads to stronger irreversibility effects, particularly in the evaporation and separation processes [20]. Similar behavior has been observed in integrated Kalina systems, where optimal performance is achieved only when temperature levels, flow conditions, and fluid composition are carefully balanced [17][18].

Overall, the results indicate that increasing evaporator temperature does not simply increase available energy, but also amplifies thermodynamic losses when operating beyond the optimal range. The simultaneous rise in heat input and energy losses confirms that system performance is governed by the balance between energy supply and irreversibility generation. Consistent with findings in recent Kalina cycle studies, improved performance is achieved through proper thermal matching and operating condition optimization, rather than by maximizing heat input alone [21]. This highlights the importance of optimizing thermal matching and operating conditions in improving the practical performance of marine waste heat recovery systems.

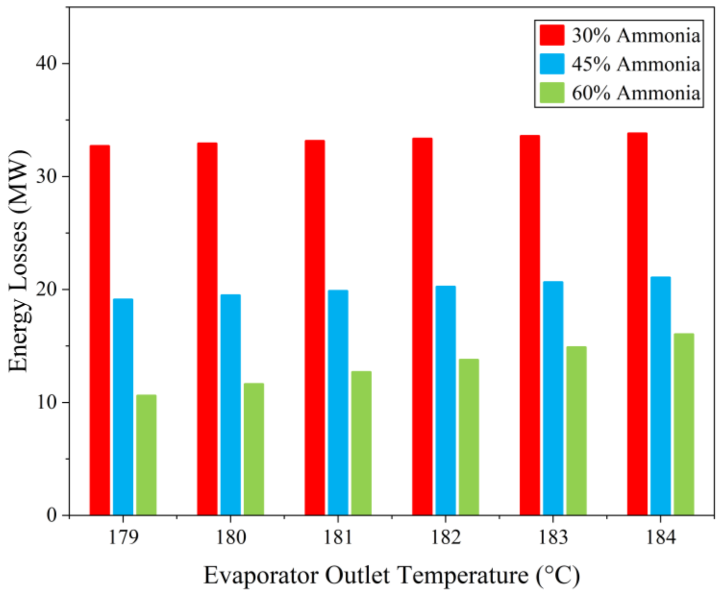


**Figure 6.** Energy losses as a function of evaporator outlet temperature at different ammonia concentrations

## IV. Conclusion

This paper evaluated the thermodynamic performance of a Kalina cycle integrated with a marine diesel engine under different ammonia-$H_2O$ concentrations and operating temperatures. The analysis covered heat input, pump work, expander work, thermal efficiency, and energy losses. The results highlight a clear relationship between fluid composition, temperature conditions, and overall cycle behavior.

1. Increasing ammonia concentration from 30% to 60% significantly reduced the required heat input, with values decreasing from 36.77 MW to 12.03 MW. This indicates that higher water content in the mixture increases the energy demand during the heating process.
2. Pump work showed relatively small variation across all conditions, ranging from 0.3684 MW to 0.3461 MW. This indicates that pump performance is mainly driven by enthalpy differences across the component rather than changes in temperature.
3. Expander work was highly sensitive to condenser temperature and ammonia concentration. The maximum output of 3.4 MW was obtained at 30% ammonia concentration and 28°C, while the lowest output of 1.72 MW was obtained at 60% ammonia concentration and 32°C. The reduction in performance is associated with a lower enthalpy during expansion as the condenser temperature increases.
4. Thermal efficiency showed a decreasing trend with increasing evaporator inlet temperature. The highest efficiency of 11.9% was achieved at 60% ammonia concentration and 179°C, while the lowest efficiency of 8.07% was observed at 30% ammonia concentration and 184°C.
5. Compared to the previous work by Feng et al [1] This study achieves an improvement of aprroximately 3.69% in thermal efficiency.
6. Energy losses increase with higher temperatures, ranging from 10.6 MW to 33.8 MW, indicating greater irreversibility at higher heat input.

Overall, the findings demonstrate that both operating temperature and ammonia-$H_2O$ composition strongly influence the thermodynamic performance of the Kalina cycle. The study also provides deeper insight into component-level energy distribution and thermodynamic losses, which may support the optimization of waste heat recovery systems in marine applications.

## Acknowledgements

The author expresses sincere gratitude to the Naval Architecture Study Program, Faculty of Engineering, Universitas Pembangunan Nasional (UPN) Veteran Jakarta, for the support and funding provided, which contributed significantly to the completion of this research.

## References

[1] Y. Feng, Z. Du, M. Shreka, Y. Zhu, S. Zhou, and W. Zhang, "Thermodynamic analysis and performance optimization of the supercritical carbon dioxide Brayton cycle combined with the Kalina cycle for waste heat recovery from a marine low-speed diesel engine," *Energy Convers. Manag.*, vol. 206, no. January, p. 112483, 2020, doi: 10.1016/j.enconman.2020.112483.

[2] International Maritime Organization (IMO), "Fourth IMO GreenHouse Gas Study 2020 Executive Summary," London, 2020.

[3] X. Yang, S. Yang, H. Wang, Z. Yu, Z. Liu, and W. Zhang, "Parametric assessment, multi-objective optimization and advanced exergy analysis of a combined thermal-compressed air energy storage with an ejector-assisted Kalina cycle," *Energy*, vol. 239, p. 122148, 2022, doi: 10.1016/j.energy.2021.122148.

[4] T. Ouyang, Z. Wang, Z. Zhao, J. Lu, and M. Zhang, "An advanced marine engine waste heat utilization scheme: Electricity-cooling cogeneration system integrated with heat storage device," *Energy Convers. Manag.*, vol. 235, no. February, p. 113955, 2021, doi: 10.1016/j.enconman.2021.113955.

[5] U. Larsen, O. Sigthorsson, and F. Haglind, "A comparison of advanced heat recovery power cycles in a combined cycle for

large ships," *Energy*, vol. 74, no. x, pp. 260–268, 2014, doi: 10.1016/j.energy.2014.06.096.

[6] T. Nguyen, T. Knudsen, U. Larsen, and F. Haglind, "Thermodynamic evaluation of the Kalina split-cycle concepts for waste heat recovery applications," *Energy*, vol. 71, pp. 277–288, 2014, doi: 10.1016/j.energy.2014.04.060.

[7] M. M. Hossain, S. Hossain, N. A. Ahmed, and M. M. Ehsan, "Energy and AI Numerical Investigation of a modified Kalina cycle system for high-temperature application and genetic algorithm based optimization of the multi-phase expander's inlet condition," *Energy AI*, vol. 6, p. 100117, 2021, doi: 10.1016/j.egyai.2021.100117.

[8] P. Bombarda, C. M. Invernizzi, and C. Pietra, "Heat recovery from Diesel engines : A thermodynamic comparison between Kalina and ORC cycles," *Appl. Therm. Eng.*, vol. 30, no. 2–3, pp. 212–219, 2010, doi: 10.1016/j.applthermaleng.2009.08.006.

[9] A. Srivastava and M. Maheshwari, "Thermodynamic analysis of solar assisted binary vapour cycle using ammonia-water mixture and transcritical CO2 : A review," vol. 10, no. 3, pp. 790–810, 2024, doi: 10.14744/thermal.0000818.

[10] M. W. Eraiby and D. F. Maki, "A Literature Review of Modification Kalina," vol. 42, no. 1, pp. 63–84, 2025.

[11] A. Intakham, A. Asanakham, T. Deethayat, and T. Kiatsiriroat, "Results in Engineering Performance analysis and optimum ammonia-water concentration of basic Kalina cycle," *Results Eng.*, vol. 26, no. August 2024, p. 104887, 2025, doi: 10.1016/j.rineng.2025.104887.

[12] D. Zhang, Y. Song, J. Gao, Z. Shen, L. Li, and A. Yao, "Research on Ship Engine Fuel Consumption Prediction Algorithm Based on Adaptive Optimization Generative Network," *J. Mar. Sci. Eng.*, vol. 13, no. 6, pp. 1–30, 2025, doi: 10.3390/jmse13061140.

[13] H. Wang, J. Wang, Z. Liu, H. Chen, and X. Liu, "Thermodynamic Analysis of a New Combined Cooling and Power System Coupled by the Kalina Cycle and Ammonia–Water Absorption Refrigeration Cycle," *Sustain. Artic.*, vol. 14, no. 20, p. 13260, 2022, [Online]. Available: https://www.mdpi.com/2071-1050/14/20/13260

[14] U. Kartal, Furkan, Ozveren, "Energy and exergy analysis of entrained bed gasifier / GT / Kalina cycle model for CO 2 co-gasification of waste tyre and biochar," vol. 331, no. September 2022, 2022, doi: 10.1016/j.fuel.2022.125943.

[15] A. Elbir, "Highly Efficient Energy Integration : Thermodynamic Analysis of Heat Recovered from SOFC Through S-CO 2 And Kalina Cycles," vol. 27, no. 4, pp. 43–55, 2024, doi: 10.5541/ijot.1486368.

[16] N. Nematzadeh, H. Ghaebi, and E. A. Aghdam, "Thermo-Economic Analysis of Innovative Integrated Power Cycles for Low-Temperature Heat Sources Based on Heat Transformer," *Sustain. Artic.*, vol. 14, p. 13194, 2022, [Online]. Available: https://doi.org/10.3390/ su142013194%0AAcademic

[17] D. Atashbozorg, A. M. Arasteh, G. Salehi, and M. T. Azad, "Analysis of Different Organic Rankine and Kalina Cycles for Waste Heat Recovery in the Iron and Steel Industry," 2022, doi: 10.1021/acsomega.2c03922.

[18] A. Pirmohamadi and B. M. Ziapour, "Heliyon Investigation of a novel multigeneration system driven by an ammonia-methane Brayton cycle with partial production and utilization of ammonia, methane, and hydrogen: Energy and carbon footprint assessments," *Heliyon*, vol. 10, no. 19, p. e38769, 2024, doi: 10.1016/j.heliyon.2024.e38769.

[19] Y. Wang, H. Yang, and K. Xu, "Thermo-economic investigation and optimization of parallel double-evaporator organic Rankine & Kalina cycles driven by the waste heat of an industrial roller kiln : A comparative study," *Energy Reports*, vol. 7, pp. 2276–2293, 2021, doi: 10.1016/j.egyr.2021.04.018.

[20] A. Pirmohamadi, H. Ghaebi, B. M. Ziapour, and M. Ebadollahi, "Exergoeconomic Analysis of a Novel Hybrid System by Integrating the Kalina and Heat Pump Cycles with a Nitrogen Closed Brayton System," *Energy Reports*, vol. 7, pp. 546–564, 2021, doi: 10.1016/j.egyr.2021.01.009.

[21] Z. Wu, L. Chen, H. Feng, and Y. Ge, "Constructal thermodynamic optimization for a novel Kalina-organic Rankine combined cycle to utilize waste heat," *Energy Reports*, vol. 7, pp. 6095–6106, 2021, doi: 10.1016/j.egyr.2021.09.025.

[22] H. Abbasi, H. Pourrahmani, N. Chitgar, and J. Van, "Thermodynamic analysis of a tri-generation system using SOFC and HDH desalination unit," *Int. J. Hydrogen Energy*, vol. 72, pp. 1204–1215, 2021, doi: 10.1016/j.ijhydene.2021.04.152.

[23] R. Akimoto, T. Yamaki, M. Nakaiwa, and K. Matsuda, "Case Studies in Thermal Engineering Evaluation of a Power Generation System that Integrates Multiple Kalina Cycles and Absorption Heat Pumps," *Case Stud. Therm. Eng.*, vol. 28, p. 101363, 2021, doi: 10.1016/j.csite.2021.101363.